

Human Stromal Cell Aggregates Concentrate Adipose Tissue Constitutive Cell Population by In Vitro DNA Quantification Analysis

Borja Sesé, Ph.D.
 Javier M. Sanmartín, M.Sc.
 Bernat Ortega, A.S.
 Ramon Llull, M.D., Ph.D.

Palma de Mallorca and Badalona,
 Spain; and Gainesville, Fla.



Background: Regenerative cell strategies rely on stromal cell implants to attain an observable clinical outcome. However, the effective cell dose to ensure a therapeutic response remains unknown. To achieve a higher cell dose, the authors hypothesized that reducing the volume occupied by mature adipocytes in lipoaspirate will concentrate the stromal vascular fraction present in the original tissue.

Methods: Human standardized lipoaspirate ($n = 6$) was centrifuged (1200 g for 3 minutes) and the water phase was discarded. Mechanical disaggregation was achieved by shearing tissue through 2.4- and 1.2-mm Luer-to-Luer transfers. After a second centrifugation (800 g for 10 minutes), stromal cell aggregates were separated from the supernatant oil phase. Lipoaspirate percentage composition was determined by its constituent weights. Cell content was measured by total DNA quantification, and partial cell viability was determined by image cytometry. Tissue sections were evaluated histologically (hematoxylin and eosin and Masson trichrome stains).

Results: Stromal cell aggregates reduced the standardized lipoaspirate mass to 28.6 ± 4.2 percent. Accordingly, the cell density increased by 222.6 ± 63.3 percent (from 9.9 ± 1.4 million cells/ g to 31.3 ± 6.6 million cells/ g ; $p < 0.05$). Cell viability was unaffected in stromal cell aggregates (71.3 ± 2.5 percent) compared to standardized lipoaspirate (72.2 ± 2.3 percent), and histologic analysis revealed high-density areas enriched with stromal cells (622.9 ± 145.6 percent) and extracellular matrix (871.2 ± 80.3 percent).

Conclusion: Stromal cell aggregates represent a biological agent that triples the cell density versus unprocessed lipoaspirate, low on oil and water fluids, and enriched extracellular matrix components. (*Plast. Reconstr. Surg.* 146: 1285, 2020.)

Adipose tissue contains a specific population of resident cells that can be divided into two defined groups: mature adipocytes (parenchyma) and a heterogeneous population of stromal cells (stroma) constituted by fibroblasts, endothelial cells, resident mononuclear cells, and progenitor cells.¹⁻³ The therapeutic potential of fat tissue appears to rely on this stromal cell population, which has been shown to respond to injury

by (1) leading extracellular matrix synthesis and remodeling, (2) promoting angiogenesis and vasculogenesis, (3) reducing inflammation through its immunomodulatory effect, and (4) repopulating the tissue with new functional cells given their multipotent capacity.⁴⁻⁷

Given the reparative capacities of stromal cells, we theorized that the therapeutic cell dose required to orchestrate a successful reparative response in any given tissue must be at least equal to the constitutive cell density present in that same

From the Cancer Cell Biology Group, Institut d'Investigació Sanitària Illes Balears; Servei de Genètica, Hospital Universitari Son Espases; Institut Català d'Oncologia, Hospital Germans Trias i Pujol; Cell Pro Tech Spain; and the University of Florida College of Medicine.

Received for publication October 11, 2019; accepted May 21, 2020.

Copyright © 2020 by the American Society of Plastic Surgeons

DOI: 10.1097/PRS.0000000000007342

Disclosure: None of the authors of this article has any financial disclosures to report.

Related digital media are available in the full-text version of the article on www.PRSJournal.com.

tissue under physiologic conditions. We defined this new therapeutic concept as the “constitutive cell dose.” Our group had previously reported that the constitutive cell density of adipose tissue is 10.5 ± 0.7 million cells/g, as determined by DNA quantification analysis, under the reported conditions.⁸ Considering this constitutive cell dose, current enzymatic dissociation methods are seen as inefficient, being able to recover only 0.68 ± 0.04 million cells/g of lipoaspirate.⁸ In recent years, mechanical disaggregation has emerged as an alternative method to overcome current limitations of enzymatic procedures associated with high costs and complications with regulatory agencies.⁹ Mechanical disaggregation of adipose tissue results in mature adipocyte breakage and stromal tissue fragmentation into reduced size particles.^{10,11} In our previous work, we have characterized mechanically disaggregated adipose tissue fragments (known as nanofat), composed of small stromal particles dispersed throughout an emulsion of oil into water. This coarse dispersion results from shear-induced adipocyte stripping and release of adipocyte fatty oil contents, and emulsification of such oil into the water phase.⁸ By definition, an emulsion is a mixture of two immiscible liquids, usually oil and water, in which one liquid is dispersed throughout the other one in the form of microscopic droplets.¹² During mechanical shearing, ruptured adipocytes release their free fatty acid content, mainly triglycerides, into the extracellular milieu along with the water fraction contained in standardized lipoaspirate. The same shear forces that disaggregate fat tissue are also responsible for the emulsification process among the oil and water phases by acting on the interface between these two immiscible fluids.¹³ Compared to enzymatic dissociation of stromal vascular fraction, our findings revealed that emulsified nanofat yielded 10 times more cells by reaching 6.6 ± 0.4 million cells/g of processed fat tissue.⁸ As opposed to enzymatically isolated cells, mechanical disaggregation results in aggregated cells that remain attached to their native extracellular matrix, preserving their microvasculature interactions, seemingly sparing viability and functional potency.^{14–16} Despite its significant improvement over enzymatic methods, mechanically disaggregated fat particles still stand below the native adipose tissue cell density, containing 7.3 ± 0.5 million cells/g.⁸ To resolve this, we speculated that removing all dispensable components from lipoaspirate, mainly oil and water, would increase the final cell density by constraining the stromal cell population from tissue fragments

into a smaller volume. However, conventional centrifugation failed to discriminate fluid from tissue phases: the density gradient between oil and water, which allows for stratification during centrifugation, becomes homogeneous by the emulsion of these two fluids, thus leaving tissue fragments dispersed across the column. Therefore, we hypothesized that removing the aqueous component from standardized lipoaspirate will avoid any later emulsification event, allowing the stratification of oil and stromal components after mechanical disaggregation. We defined the resulting tissue fraction as stromal cell aggregates because it represents the entire stromal component of adipose tissue (stromal cells and extracellular matrix), nearly stripped of its parenchymal counterpart (destroyed adipocytes) and aqueous contaminants from the liposuction (including remnants of tumescent fluid). In this study, we present a detailed method and provide the scientific rationale behind the isolation of the stromal component from adipose tissue based on a mechanical disaggregation protocol.

PATIENTS AND METHODS

Adipose Tissue Harvesting

The present study was authorized by the Ethics Committee of the Balearic Isles. All liposuctions were performed under general anesthesia and informed consent documents were signed by all patients. Lipoaspirate was obtained from six healthy patients. Patients were all female and ranged from 18 to 45 years of age, with a body mass index of 21.5 ± 2.0 kg/m². Tumescent fluid (INIBSACAIN Plus 0.05%; Inisba Hospital, Barcelona, Spain) was infiltrated at the abdominal area using a tumescent infiltrator cannula (Tulip Medical Products, San Diego, Calif.). Forty cubic centimeters of lipoaspirate was harvested using a Carraway Harvester cannula (Tulip Medical) into 20-cc syringes with a Johnnie Lok (Tulip Medical) installed to hold suction. Lipoaspirate was transferred into a fat press (Tulip Medical) and standardized by washing with an equal volume of saline solution by hand rocking eight to 10 times. Fluids were expelled by manual pressure, and standardized lipoaspirate was collected into 20-cc syringes.

Mechanical Disaggregation of Stromal Cell Aggregates

Standardized lipoaspirate was centrifuged at 1200 *g* for 3 minutes using the Coleman technique, resulting in a negligible oil phase at the

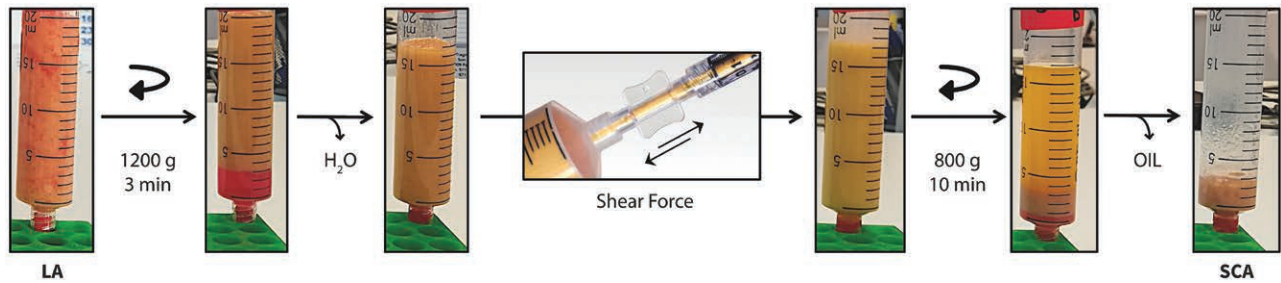


Fig. 1. Mechanical disaggregation and isolation of stromal cell aggregates. Standardized lipoaspirate (left) was centrifuged at 1200 g for 3 minutes and the water phase was discarded (second from left) to obtain Coleman fat (third from left). Mechanical disaggregation by shear forces caused stromal tissue fragmentation and a major adipocyte breakage (third from right). After a second centrifugation at 800 g for 10 minutes, the oil phase was discarded (second from right) to obtain stromal cell aggregates as a final product (right). LA, lipoaspirate; SCA, stromal cell aggregates.

top, fat tissue in the middle, and an aqueous phase at the bottom.¹⁷ The aqueous phase was expelled through the syringe and discarded (the aqueous phase remained fairly constant, indicating sample standardization of physical components). The fat-containing syringe was sequentially passed 30 times through 2.4- and 1.2-mm Luer-to-Luer transfer (Tulip Medical) connected to another empty 20-cc syringe. Mechanically disaggregated fat tissue was centrifuged at 800 g for 10 minutes, resulting in a transparent oil phase at the top and stromal cell aggregates at the bottom. The oil phase was discarded by decantation, and stromal cell aggregates were transferred into another empty 20-cc syringe (Fig. 1).

Enzymatic Dissociation of Stromal Vascular Fraction

Standardized lipoaspirate and stromal cell aggregates were transferred into a 50-ml tube and incubated at 37°C for 40 minutes under continuous agitation with an equal volume of digestion buffer containing 200 collagen digestion units/ml dissociation enzyme (GIDzyme-2; GID Bio Inc., Louisville, Colo.). Enzymatic activity was stopped with human albumin (2.5% final concentration), and the cell suspension was centrifuged at 800 g for 10 minutes. The supernatant was discarded and the resulting cell pellet (stromal vascular fraction) was resuspended and filtered through a 100- μ m mesh.

Lipoaspirate Mass Percentage Composition Analysis

During mechanical disaggregation of stromal cell aggregates, the main components of standardized lipoaspirate (i.e., water, oil, and stromal cell aggregates) were sequentially separated and collected into previously tared (empty weight)

50-ml tubes. A standardized lipoaspirate-containing syringe was also tared in advance. We measured the gross weight (total weight) of each tube and syringe using a semimicro balance (Radwag, Radom, Poland). By subtracting the tare weight from the gross weight, we obtained the net weight of each sample. To determine the mass percentage composition, the net weight of each fraction was divided by the net weight of standardized lipoaspirate and multiplied by 100.

Cell Number Quantification by Total DNA Analysis

Cell number quantification was performed as described by Sesé et al.⁸ Briefly, 50 to 100 mg of standardized lipoaspirate and stromal cell aggregates was placed into a sterile 1.5-ml Eppendorf (Eppendorf AG, Hamburg, Germany) tube. A known isolated, unclustered, stromal vascular fraction cell pellet was used as a reference control. The DNA extraction was performed following the manufacturer's instructions (E.Z.N.A. tissue DNA Kit; Promega, Madison, Wis.). DNA content was measured by Nanodrop (Thermo Fisher Scientific, Waltham, Mass.) quantification. Cell numbers from test specimens were interpolated from the DNA-to-cell ratio obtained from the reference control sample.

Cell Viability Quantification by Image Cytometry

Cell viability was performed on stromal vascular fraction cell suspensions from each specimen (standardized lipoaspirate and stromal cell aggregates) by an automated NucleoCounter NC-3000 (ChemoMetec, Allerød, Denmark). Stromal vascular fraction cell suspension was filtered using a 100- μ m cell strainer and loaded into a Vial-Cassette (ChemoMetec). Cell viability was automatically determined in 30 to 40 seconds.

Histologic Analysis

Standardized lipoaspirate and stromal cell aggregates were placed directly into plastic cassettes. All samples were fixed in 4% paraformaldehyde, dehydrated, and embedded in paraffin. Paraffin blocks were sent to the histopathology facility at the Institute for Research in Biomedicine (IRB Barcelona, Barcelona, Spain), sectioned at 3- μ m thickness, and stained with hematoxylin and eosin and Masson trichrome standard protocols. Brightfield images were acquired with a NanoZoomer-2.0 HT C9600 digital scanner (Hamamatsu Photonics, Hamamatsu, Japan) at two different magnifications. For quantitative analysis of histologic sections, three randomly selected areas from paired standardized lipoaspirate and stromal cell aggregate samples were processed using the software ImageJ (National Institutes of Health, Bethesda, Md.). Cell content quantification was performed on hematoxylin and eosin-stained sections by manual nuclei counting using the multipoint tool. Collagen levels were analyzed on Masson trichrome-stained sections (blue stain) by measuring the integrated density, the sum of pixel intensities on a gray scale, of highlighted collagen area. Integrated density values are represented as optical density. Filter retentate samples were processed and stained with hematoxylin and eosin as described by Purohit.¹⁸ Brightfield images were acquired using a Moticam 1080 FullHD camera (Motic, Hong Kong) and Motic Image Plus 2.0 software at 100 \times magnification.

Statistical Analysis

Bar graphs are represented as mean \pm SEM and box plots represent the median, mean, and minimum and maximum values. Statistical analyses were performed using GraphPad Prism software version 7.0a (GraphPad Software, Inc., San Diego, Calif.). Paired *t* tests were used to analyze cell density and viability of standardized lipoaspirate versus stromal cell aggregate samples. Unpaired *t* tests were used to analyze cell count and collagen levels of standardized lipoaspirate versus stromal cell aggregate histologic sections. Values of *p* < 0.05 were considered statistically significant.

RESULTS

Stromal Tissue Represents Almost One-Third of Standardized Lipoaspirate Total Mass

To evaluate the composition of standardized lipoaspirate, we determined the mass percentage of its main constituents: water, oil, and tissue. After stromal cell aggregate isolation, we measured the net weight of each fraction (water, oil, and stromal

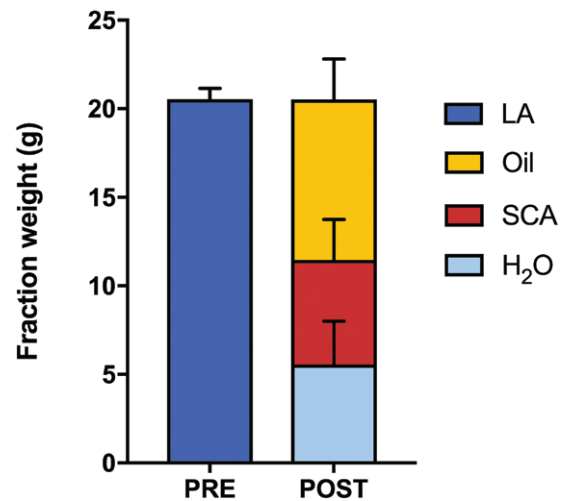


Fig. 2. Tissue fraction of standardized lipoaspirate components. Bar graphs show the fraction weight before (*PRE*) and after (*POST*) fat tissue processing (*n* = 6). Pre-fat tissue processing samples represent the initial standardized lipoaspirate, and post-fat tissue processing samples contain the combination of oil, water, and stromal components. Values are represented as mean \pm SEM. LA, lipoaspirate; OIL, oil phase; H₂O, water phase; SCA, stromal cell aggregates.

cell aggregates) and calculated their mass percentage composition relative to the original net weight of unprocessed standardized lipoaspirate. Starting with 20.5 \pm 0.6 g of standardized lipoaspirate, we obtained values of 27.4 \pm 5.1 percent water (5.5 \pm 1.0 g), 43.9 \pm 4.0 percent oil (9.0 \pm 0.9 g), and 28.6 \pm 4.2 percent stromal cell aggregates (5.9 \pm 4.2 g). These results indicate that approximately one-third of standardized lipoaspirate content is made of stromal tissue (Fig. 2).

Stromal Cell Aggregates Concentrate Standardized Lipoaspirate Cell Density by Three-Fold

To evaluate the cell density contained in mechanically isolated stromal cell aggregates, we determined the total nucleated cells based on DNA tissue content as described previously.⁸ Based on DNA analysis, the cell density of stromal cell aggregates was 31.3 \pm 6.6 million cells/g, whereas unprocessed standardized lipoaspirate presented 9.9 \pm 1.4 million cells/g (Fig. 3), confirming our previous report.⁸ Our results indicate that isolated stromal cell aggregates presented a cell density three times more concentrated than original standardized lipoaspirate samples, reflected as a 222.6 \pm 63.3 percent increase in their cell density population.

Mechanically Dissociated Stromal Cell Aggregates Contain Viable Cells

The viability of cells present in stromal cell aggregates was analyzed by image cytometry

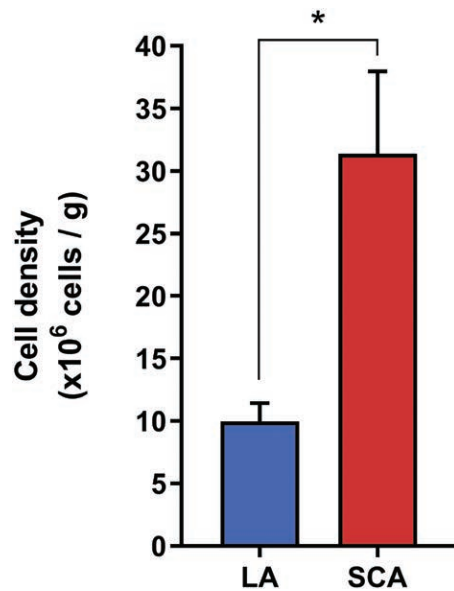


Fig. 3. Cell content of standardized lipoaspirate and stromal cell aggregates. Bar graphs show the cell density of different specimens as the number of cells $\times 10^6$ per gram of sample ($n = 4$). Values are represented as mean \pm SEM and statistical analysis was performed using a paired t test ($*p < 0.05$). LA, lipoaspirate; SCA, stromal cell aggregates.

on enzymatically dissociated cells from stromal cell aggregates and standardized lipoaspirate samples following a stromal vascular fraction isolation protocol. On enzymatic dissociation, the viability of isolated cells was 72.2 ± 2.3 percent for unprocessed standardized lipoaspirate and 71.3 ± 2.5 percent for stromal cell aggregate preparations (Fig. 4). These results indicate that the absence of water fraction during mechanical disaggregation had no impact on cell viability. Also, these results support our previous findings on the viability of nanofat cell aggregates.⁸

Histologic Analysis of Stromal Cell Aggregates Revealed an Enrichment in Stromal Cell Density and Extracellular Collagen, and a Depletion of the Mature Adipocyte Population

To verify whether isolated stromal cell aggregates concentrate the cell density from original standardized lipoaspirate, we performed histologic analysis to evaluate the cell content and extracellular matrix composition in hematoxylin and eosin- and Mason trichrome-stained sections, respectively. As shown by hematoxylin and eosin staining, unprocessed standardized lipoaspirate (Fig. 5, above) presented a well-organized structure of packed mature adipocytes associated with a network of connective tissue

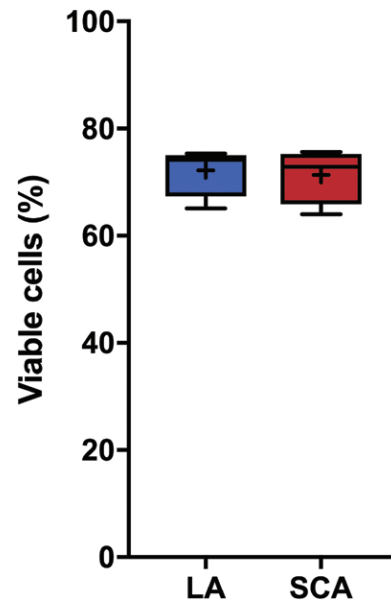


Fig. 4. Cell viability of stromal cell aggregates. Both standardized lipoaspirate and stromal cell aggregates were enzymatically dissociated to analyze the cell viability of stromal vascular fraction cells. Values are represented as the percentage of viable cells in the stromal vascular fraction from each sample ($n = 4$). The boxes show the interquartile range (from lower to upper quartiles) of viable cells, including the median (middle quartile) and mean (asterisk). The whiskers show the location of the minimum and maximum values of all the data. Statistical analysis was performed using a paired t test ($p =$ not significant). LA, lipoaspirate; SCA, stromal cell aggregates.

where stromal cells are located, suspended in the extracellular fluid containing significant oil droplets. In contrast, stromal cell aggregates (Fig. 5, below) showed regions harboring a massive concentration of stromal cell density as a result of (1) absent and fractured mature adipocytes after mechanical disaggregation and (2) removal of aqueous and oil content. Nuclei count on these high-density regions showed a 622.9 ± 145.6 percent increase in the cell population of stromal cell aggregates compared to standardized lipoaspirate. Mason trichrome staining also presented enriched areas of connective tissue that co-localize with high-density cell regions in stromal cell aggregates. Integrated density analysis revealed an increase of collagen levels by 871.2 ± 80.3 percent in stromal cell aggregates compared with standardized lipoaspirate. These findings provide a visual indication of the concentrated state of stromal cell aggregates. [See Figure, Supplemental Digital Content 1, which shows quantification of standardized lipoaspirate and stromal cell aggregate histologic sections using ImageJ. Representative histologic sections

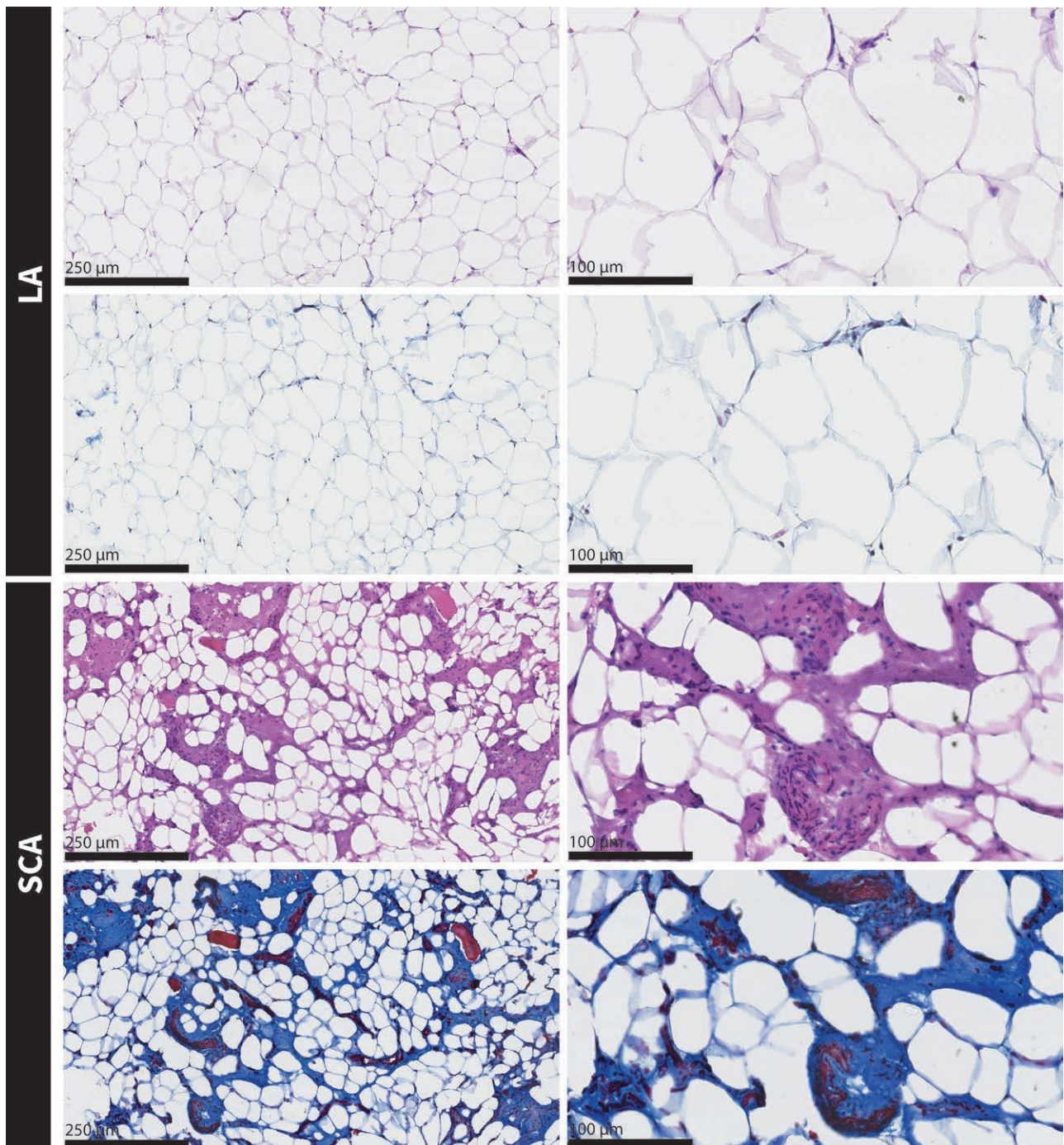


Fig. 5. Histologic analysis of standardized lipoaspirate and stromal cell aggregates by hematoxylin and eosin (*above*) and Masson trichrome (*below*) staining. Representative histologic sections are shown at two different magnifications: scale bars = 250 μm (*left*) and 100 μm (*right*). LA, lipoaspirate; SCA, stromal cell aggregates.

are shown (scale bar = 250 μm). (*Left*) Point selection with a numeric label represents stained nuclei counts on hematoxylin and eosin sections. Cell count was performed manually ($n = 3$). (*Right*) Areas highlighted in red represent stained collagen on Masson trichrome–stained sections. Collagen quantification was analyzed

by integrated density analysis (number of pixels \times intensity of pixels) and represented as optical density ($n = 3$). Values are represented as mean \pm SEM, and statistical analysis was performed using unpaired t tests ($*p < 0.05$; $***p < 0.001$). LA, lipoaspirate; SCA, stromal cell aggregates; OD, optical density, <http://links.lww.com/PRS/E250>.]

DISCUSSION

A clear understanding of the biological components behind adipose tissue–derived implants is a critical goal for cell and regenerative therapies. Here, we describe an alternative mechanical disaggregation protocol to improve the implant's cell density by simply reducing the volume of processed fat tissue while retaining the same number of cells.¹⁹ Similarly, Yao et al. and Pallua et al. have achieved a similar product named “ECM/SVF gel” and “lipoconcentrate,” respectively, although they performed one last filtration step to remove larger connective tissue fragments. We deliberately avoided this last filtering step, as these connective tissue fibers retained inside the filter contained a high density of stromal cells, which may be beneficial from a therapeutic standpoint. [See **Figure, Supplemental Digital Content 2**, which shows histologic analysis of stromal fragments retained by the filter. Retentate of stromal fragments after filtering stromal cell aggregates within the oil phase is shown (*left*). Squash smear of stromal fragments showing a high density of stromal cells by hematoxylin and eosin staining at 100× magnification (*right*), <http://links.lww.com/PRS/E251>.] As a downside, we were not able to inject stromal cell aggregates through finer needles (25- and 27-gauge) given the size of stromal fragments.

By reducing the standardized lipoaspirate mass to 28.6 ± 4.2 percent and retaining the majority of stromal vascular fraction present in the original tissue, stromal cell aggregates increased the cell density by 222.6 ± 63.3 percent (**Figs. 2 and 3**). The fact that stromal cell aggregates triplicated the cell density of standardized lipoaspirate was a direct consequence of reducing their mass by one-third. To support these findings, histologic analysis of stromal cell aggregates revealed a large number of cells concentrated into high-density areas enriched with extracellular matrix components (**Fig. 5**). Also, the shearing process in the absence of an aqueous phase did not affect cell viability when measured in the enzymatically dissociated fraction of stromal cell aggregates (**Fig. 4**). Besides, this study presents some methodologic limitations that should be noted. First, we are aware that our cell content analysis of stromal cell aggregates may include some DNA released from broken adipocytes before tissue DNA extraction. Nevertheless, because it has been geometrically estimated that 1 cc of standardized lipoaspirate contains approximately 1 million adipocytes, and assuming that 1 cc is approximately equivalent to 1 g of lipoaspirate, erroneous quantification of dead adipocytes would have overestimated our cell density by only 10 percent, which

would not affect the relevance of our findings.²⁰ Second, cell viability analysis of enzymatically isolated cells represents less than 7 percent of the total tissue cell content, meaning that more than 90 percent remain undetermined.⁸ Unfortunately, there are still no reliable methods to determine the cell viability from whole tissue samples.^{21,22} Thus, rather than make our viability claims extensive to the entire tissue, we aimed to observe differences in cell viability before (standardized lipoaspirate) and after (stromal cell aggregates) mechanical disaggregation under the same conditions.

Recent evidence suggests that the number of transplanted cells and their concentration play a pivotal role in clinical responses to different therapeutic approaches.^{23–25} However, the optimal dose for stromal cell application in several cell-based therapies remains unknown.^{25,26} We anticipate that the minimal dose required to obtain a therapeutic effect must be equivalent and likely far superior to the cell population present in adipose tissue under normal conditions, the so-called constitutive cell dose (i.e., 10.5 ± 0.7 million cells/g).⁸ **Figure 6** illustrates the resulting products derived from different methods of adipose tissue processing. Despite their low cell yield when compared to stromal aggregates, enzymatically isolated stromal vascular fraction cells still represent a safe option for intravenous delivery.^{14–16} Previous nanofat-generating methods caused a 30 percent loss of adipose tissue cell density, resulting in 70 percent of the constitutive cell dose ($0.7 \times$ constitutive cell dose).⁸ The fact that nanofat can be injected through relatively small-bore needles makes it a suitable candidate in small-volume regenerative applications.^{27–29} In contrast, although requiring a larger needle bore, stromal cell aggregates increased the cell population described in native adipose tissue by 200 percent, reaching a cell density three times beyond the constitutive cell dose, free of oil and water volume.

Considered together, stromal cell aggregates may have potential use in tissue repair and regeneration, intended for site-specific intralesional delivery, especially for wound healing applications, although it has yet to be clinically proven. Most importantly, another advantage of stromal cell aggregates is the absence of fat cells and their oil content, which could prevent severe complications such as tissue necrosis and the formation of oil cysts.^{30–32} Furthermore, because isolated stromal vascular fraction cells have already shown clinical improvement in patients with knee osteoarthritis, we believe that stromal cell aggregates could improve current treatments for joint disorders by means of intraarticular injection with better clinical

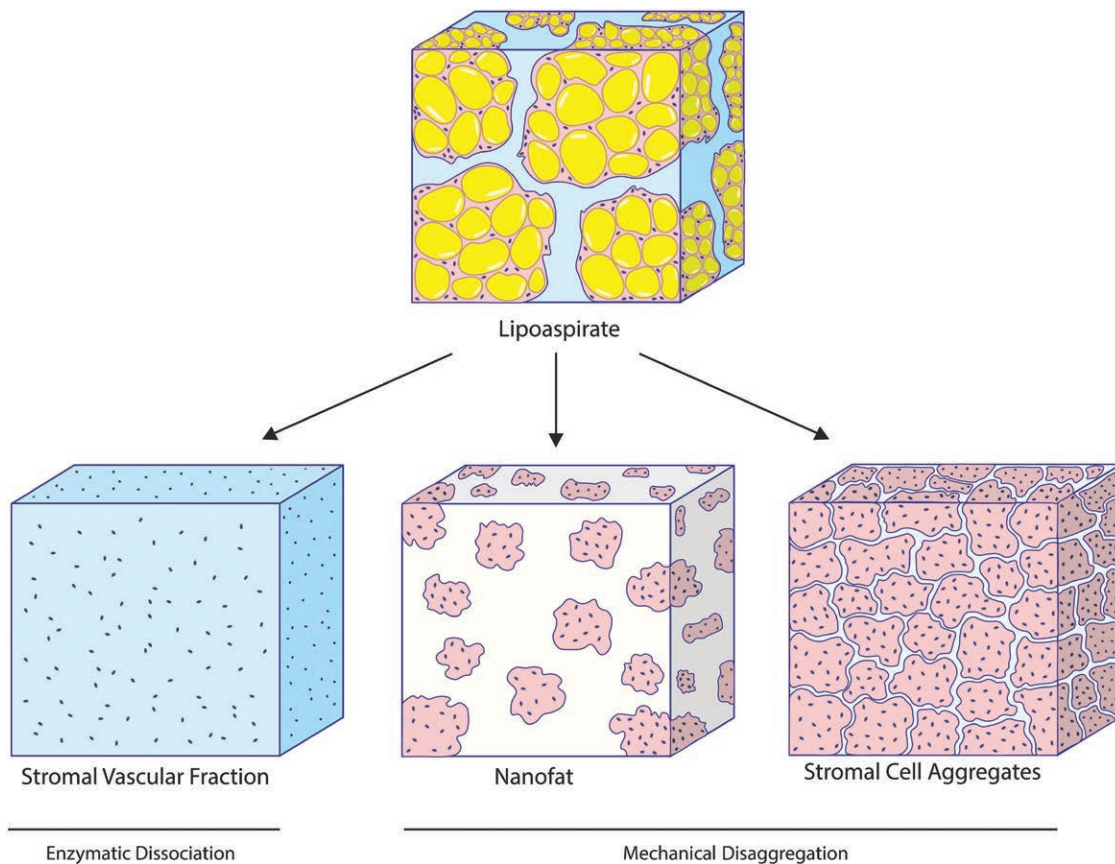


Fig. 6. Schematic representation of 1 cc of different products obtained from adipose tissue processing. Lipoaspirate contains adipose tissue fragments (adipocytes, stromal cells, and extracellular matrix) within an aqueous phase. Stromal vascular fraction consists of isolated cells (stromal cells) resuspended in a suitable volume of saline solution. Nanofat presents cell aggregates (stromal cells and extracellular matrix) immersed in an emulsion of oil and water. Stromal cell aggregates (stromal cells and extracellular matrix) constitute a concentrate of aggregated cells free of oil and water contaminants. *ECM*, extracellular matrix.

results.^{33,34} To validate a better performance over isolated cells in tissue repair, further studies are needed to test the potency of stromal cell aggregates in (1) collagen synthesis and remodeling, (2) formation of new blood vessels, and (3) regulation of nonspecific immune responses.

CONCLUSIONS

In recent years, the use of stromal cells derived from adipose tissue has been increasingly adopted by clinicians in regenerative applications. Despite some promising results, the effective cell dose leading to a therapeutic response remains unsolved. In this work, we present a simple method to concentrate the stromal vascular fraction from adipose tissue by reducing the volume occupied by mature adipocytes. Lipoaspirate was fragmented into stromal cell aggregates after mechanical shearing and separated from water and oil fractions after a two-step centrifugation protocol. These stromal cell

aggregates constitute a biological agent that triplicates the cell density present in native adipose tissue based on DNA quantification analysis. Also, our data show high-density areas enriched with extracellular matrix components. Although further studies are necessary to validate their potential therapeutic effect, we foresee stromal cell aggregates as a powerful product for tissue repair and regeneration.

Ramon Llull, M.D., Ph.D.

Cell Pro Tech Spain

Camí dels reis 308, Lab D04

Palma de Mallorca, Spain 07010

ramonllull@mac.com

Instagram: [dr.ramonllullplastica](https://www.instagram.com/dr.ramonllullplastica)

REFERENCES

1. Bluguermann C, Wu L, Petrigliano F, McAllister D, Miriuka S, Evseenko DA. Novel aspects of parenchymal-mesenchymal interactions: From cell types to molecules and beyond. *Cell Biochem Funct.* 2013;31:271–280.

2. Braga Osorio Gomes Salgado AJ, Goncalves Reis RL, Jorge Carvalho Sousa N, et al. Adipose tissue derived stem cells secretome: Soluble factors and their roles in regenerative medicine. *Curr Stem Cell Res Ther*. 2010;5:103–110.
3. Kapur SK, Katz AJ. Review of the adipose derived stem cell secretome. *Biochimie* 2013;95:2222–2228.
4. Hyldig K, Riis S, Pennisi C, Zachar V, Fink T. Implications of extracellular matrix production by adipose tissue-derived stem cells for development of wound healing therapies. *Int J Mol Sci*. 2017;18:1167.
5. Zhao L, Johnson T, Liu D. Therapeutic angiogenesis of adipose-derived stem cells for ischemic diseases. *Stem Cell Res Ther*. 2017;8:125.
6. Zhao Q, Ren H, Han Z. Mesenchymal stem cells: Immunomodulatory capability and clinical potential in immune diseases. *J Cell Immunother*. 2016;2:3–20.
7. Zuk PA, Zhu M, Mizuno H, et al. Multilineage cells from human adipose tissue: Implications for cell-based therapies. *Tissue Eng*. 2001;7:211–228.
8. Sesé B, Sanmartín JM, Ortega B, Matas-Palau A, Llull R. Nanofat cell aggregates: A near constitutive stromal cell inoculum for regenerative site-specific therapies. *Plast Reconstr Surg*. 2019;144:1079–1088.
9. Bora P, Majumdar AS. Adipose tissue-derived stromal vascular fraction in regenerative medicine: A brief review on biology and translation. *Stem Cell Res Ther*. 2017;8:145.
10. Alexander RW. Understanding mechanical emulsification (nanofat) versus enzymatic isolation of tissue stromal vascular fraction (tSVF) cells from adipose tissue: Potential uses in bio-cellular regenerative medicine. *J Prolother*. 2016;8:e947–e960.
11. Tonnard P, Verpaele A, Peeters G, Hamdi M, Cornelissen M, Declercq H. Nanofat grafting: Basic research and clinical applications. *Plast Reconstr Surg*. 2013;132:1017–1026.
12. Khan AY, Talegaonkar S, Iqbal Z, Ahmed FJ, Khar RK. Multiple emulsions: An overview. *Curr Drug Deliv*. 2006;3:429–443.
13. Tadros TF. Emulsion formation, stability, and rheology. In: Tadros TF, ed. *Emulsion Formation and Stability*. Weinheim, Germany: Wiley-VCH Verlag; 2013:1–75.
14. Bayoussief Z, Dixon JE, Stolnik S, Shakesheff KM. Aggregation promotes cell viability, proliferation, and differentiation in an in vitro model of injection cell therapy. *J Tissue Eng Regen Med*. 2012;6:e61–e73.
15. Lei X, Deng Z, Duan E. Uniform embryoid body production and enhanced mesendoderm differentiation with murine embryonic stem cells in a rotary suspension bioreactor. In: Turksen K, ed. *Bioreactors in Stem Cell Biology*. New York: Springer; 2016:63–75.
16. Goh SK, Olsen P, Banerjee I. Extracellular matrix aggregates from differentiating embryoid bodies as a scaffold to support ESC proliferation and differentiation. *PLoS One* 2013;8:e61856.
17. Coleman SR. Facial recontouring with lipostucture. *Clin Plast Surg*. 1997;24:347–367.
18. Purohit MR. Squash cytology in neurosurgical practice: A useful method in resource-limited setting with lack of frozen section facility. *J Clin Diagn Res*. 2014;8:FC09–FC12.
19. Kokai L, Rubin JP. Discussion: Nanofat cell aggregates: A nearly constitutive stromal cell inoculum for regenerative site-specific therapies. *Plast Reconstr Surg*. 2019;144:1091–1092.
20. Suga H, Matsumoto D, Inoue K, et al. Numerical measurement of viable and nonviable adipocytes and other cellular components in aspirated fat tissue. *Plast Reconstr Surg*. 2008;122:103–114.
21. Riss TL, Moravec RA, Niles AL, Duellman S, Benink HA. Cell viability assays. Available at: <https://www.ncbi.nlm.nih.gov/books/NBK144065/?report=reader>. Accessed June 1, 2018.
22. Riss TL. Is your MTT assay really the best choice? Available at: <https://www.promega.com/resources/pubhub/is-your-mtt-assay-really-the-best-choice/>. Accessed June 1, 2018.
23. Florea V, Rieger AC, DiFede DL, et al. Dose comparison study of allogeneic mesenchymal stem cells in patients with ischemic cardiomyopathy (the TRIDENT study). *Circ Res*. 2017;121:1279–1290.
24. Galipeau J, Sensébé L. Mesenchymal stromal cells: Clinical challenges and therapeutic opportunities. *Cell Stem Cell* 2018;22:824–833.
25. Xu JY, Cai WY, Tian M, Liu D, Huang RC. Stem cell transplantation dose in patients with acute myocardial infarction: A meta-analysis. *Chronic Dis Transl Med*. 2016;2:92–101.
26. Golpanian S, Schulman IH, Ebert RF, et al.; Cardiovascular Cell Therapy Research Network. Concise review: Review and perspective of cell dosage and routes of administration from preclinical and clinical studies of stem cell therapy for heart disease. *Stem Cells Transl Med*. 2016;5:186–191.
27. Bhooshan LS, Devi MG, Aniraj R, Binod P, Lekshmi M. Autologous emulsified fat injection for rejuvenation of scars: A prospective observational study. *Indian J Plast Surg*. 2018;51:77–83.
28. Kemaloğlu CA. Nanofat grafting under a split-thickness skin graft for problematic wound management. *SpringerPlus* 2016;5:138.
29. Wei H, Gu SX, Liang YD, et al. Nanofat-derived stem cells with platelet-rich fibrin improve facial contour remodeling and skin rejuvenation after autologous structural fat transplantation. *Oncotarget* 2017;8:68542–68556.
30. Yoshimura K, Coleman SR. Complications of fat grafting: How they occur and how to find, avoid, and treat them. *Clin Plast Surg*. 2015;42:383–388, ix.
31. Duong MN, Geneste A, Fallone F, Li X, Dumontet C, Muller C. The fat and the bad: Mature adipocytes, key actors in tumor progression and resistance. *Oncotarget* 2017;8:57622–57641.
32. Del Vecchio DA, Villanueva NL, Mohan R, et al. Clinical implications of gluteal fat graft migration: A dynamic anatomical study. *Plast Reconstr Surg*. 2018;142:1180–1192.
33. Yokota N, Hattori M, Ohtsuru T, et al. Comparative clinical outcomes after intra-articular injection with adipose-derived cultured stem cells or noncultured stromal vascular fraction for the treatment of knee osteoarthritis. *Am J Sports Med*. 2019;47:2577–2583.
34. Daniel Santa Maria JRG. Use of autologous adipose-derived stromal vascular fraction to treat osteoarthritis of the knee: A feasibility and safety study. *J Regen Med*. 2014;4.